THE JOURNAL OF PHYSICAL CHEMISTRY B

Article

pubs.acs.org/JPCB

Ab Initio Prediction of Proton NMR Chemical Shifts in Imidazolium Ionic Liquids

Su Chen, R. Vijayaraghavan, Douglas R. MacFarlane, and Ekaterina I. Izgorodina*

School of Chemistry, Monash University, Wellington Road, Clayton, VIC, Australia 3800

Supporting Information

ABSTRACT: The family of ionic liquids (ILs) containing 1-alkyl-3-methyl-imidazolium cations have been broadly investigated due to the simplicity of their synthesis and relatively low viscosity. Nuclear magnetic resonance (NMR) studies indicate that the proton chemical shift of the H2 proton is very sensitive to interactions between the imidazolium ring and surrounding anions and can be used as a probe of the IL structure and solute interactions that perturb this structure. In this work, we have calculated proton NMR chemical shifts of a number of ionic liquids incorporating the 1-ethyl-3-methyl-imidazolium cation and anions such as chloride, tetrafluoroborate, hexafluorophosphate, acetate, trifluoroacetate, dicyanamide, ethylsulfate, and tosylate using a number of wavefunction-based methods such as HF and MP2 as well as density functional theory. Proton NMR chemical shifts in the cation were calculated for single ion pairs with the view of (1) determining the best quantum chemical method for the accurate prediction of ^{1}H NMR chemical shifts and (2) understanding the influence on the H2 proton chemical shift of the two energetically preferable ion-pair configurations of the anion interacting with the cation, either from above the imidazolium ring or in the plane of the C2−H bond.

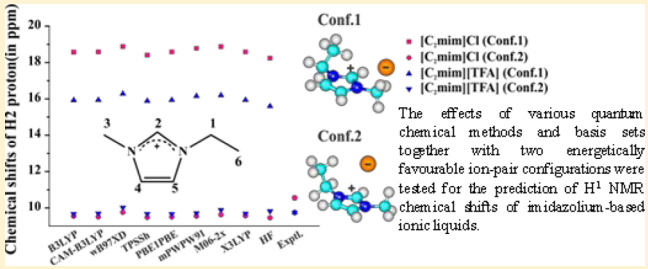

INTRODUCTION

Room-temperature ionic liquids (RTILs) are considered to be among the most promising electrolytes in a range of devices including batteries and dye-sensitized solar cells to replace volatile organic solvents due, in some cases, to their thermal stability, nonflammability, low vapor pressure, and low toxicity.[1,2] To date, the family of ILs containing 1,3-dialkyl-imidazolium cations have been extensively studied due to their desirable transport properties, especially their relatively low viscosity.[3−5] A number of experimental and theoretical studies of imidazolium-based ILs have focused on understanding the relationship between the chemical structure and the transport properties[6−13] with the view of designing novel ILs for applications in energy generation and storage devices. Many studies confirm that the chemical structure of these ILs has a significant influence on their transport properties.[7,8,10,14] For example, Every et al. reported that increasing the length of the alkyl chain on the imidazolium cation (from methyl to *n*-heptyl) led to a decrease in the melting point, conductivity, and diffusion coefficients of the cations.[8] Bonhôte et al. showed that, compared with 1-ethyl-3-methylimidazolium bis{trifluoromethylsulfonyl}amide ($[C_2mim][NTf_2]$), 1-ethyl-2,3-methylimidazolium bis{trifluoromethylsulfonyl}amide ($[C_2m_2im][NTf_2]$) with the C2 position methylated (see Figure 1) had a much higher viscosity, and they speculated that the hydrogen bonding suppression in that position led to the increase in viscosity.[10] A number of theoretical studies have been performed to further explore this unusual behavior.[11−13] Recently, in our group it was shown that the methylation at the C2 position blocked the hydrogen bond formation between the cation and the anion and resulted in high potential energy barriers between the energetically preferable ion-pair configurations on the potential energy surface, thus restricting the ion movement and leading to higher viscosity.[9] These insights are important steps in understanding the structure−property relationships that would lead to the discovery of low viscosity ILs. Equally important in this endeavor is the availability of structure-probing techniques such as IR spectroscopy,[15] dielectric spectroscopy,[16] and NMR that can probe the presence of desirable structures. However, it remains unclear how changes in the local environment that produce low-energy pathways for transport would be revealed in such spectroscopic measurements.

Nuclear magnetic resonance (NMR) is one of the most powerful tools available to investigate interionic interactions between the imidazolium ring and anion, as the proton chemical shift of the H2 proton (see Figure 1 for numbering scheme) has been found to be very sensitive to these interactions.[10,17,18] Hydrogen bond formation was associated with a downfield H2 chemical shift.[10] Thus, changes in the ^{1}H NMR chemical shits due to the interactions with the H2 proton can help us understand more clearly the effect of the local environment on transport properties of ILs. Suarez et al. compared the ^{1}H and ^{13}C NMR spectra of 1-butyl-3-

Received: October 17, 2012
Revised: February 22, 2013
Published: February 22, 2013

   dx.doi.org/10.1021/jp310267x | *J. Phys. Chem. B* 2013, 117, 3186−3197

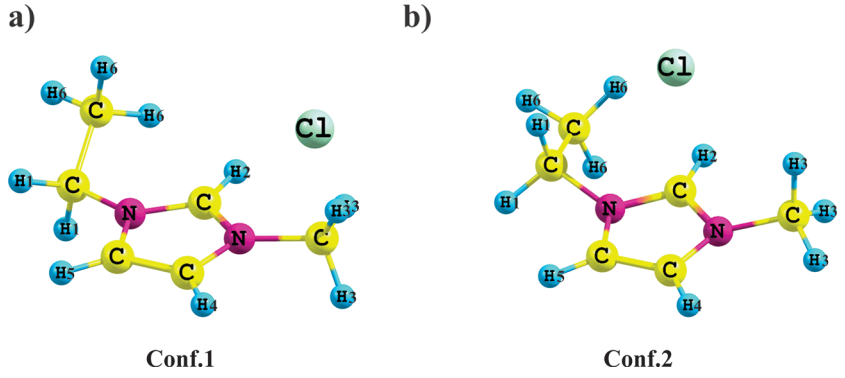

Figure 1. Energetically favorable configurations of ion pairs of imidazolium-based ILs: (a) Conf. 1, in which the anion interacts in the C2−H plane, (b) Conf. 2, in which the anion interacts above the imidazolium ring.

Scheme 1. Structures of the Cation and Anions Studied

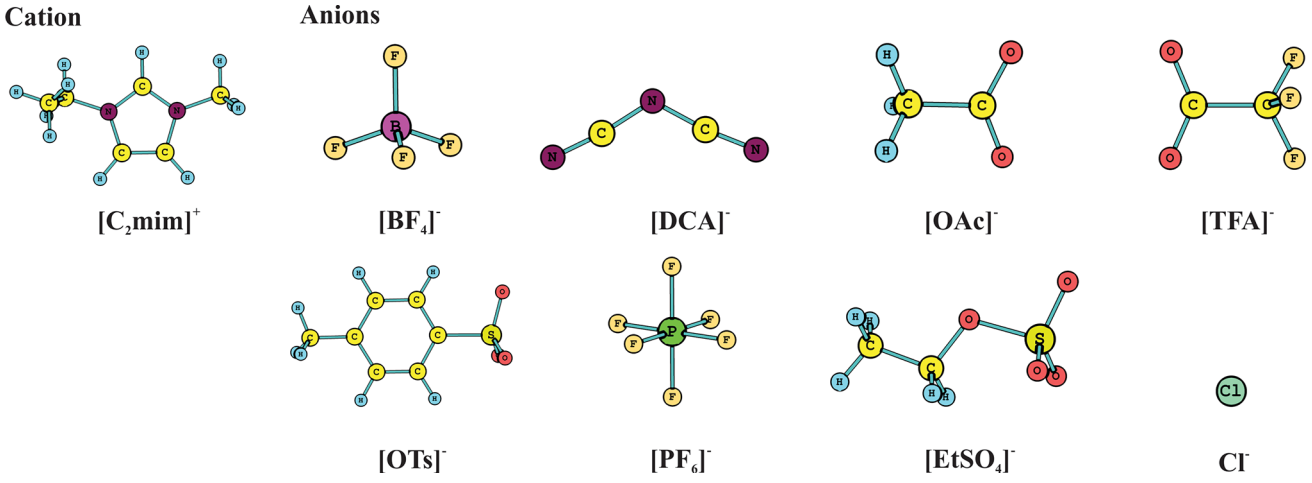

methylimidazolium tetrafluoroborate, [C_4mim][BF_4], and 1-butyl-3-methylimidazolium hexafluorophosphate, [C_4mim]-[PF_6], with that of [C_4mim]Cl and found that the chemical shift of the H2 proton in both [C_4mim][BF_4] and [C_4mim]-[PF_6] moved significantly downfield compared to that of [C_4mim]Cl, suggesting that the anion plays a major role in determining the H2 chemical shift.[19] Holbrey and Seddon studied a series of 1-alkyl-3-methylimdazolium ([$C_n$mim][BF_4] with n = 0−18) in deuterated propanone and found that the NMR peaks of the H2 proton changed only slightly, which indicated that the H2 chemical shift was relatively insensitive to increasing alkyl chain length.[20] However, the chemical factors that affect proton chemical shifts of the imidazolium ring are still ambiguous. Therefore, in this work we set out to calculate ^{1}H NMR chemical shifts of a series of imidazolium-based ILs by means of quantum chemical methods to study the structural and energetic factors that affect chemical shifts of the protons, especially the H2 proton.

NMR Chemical Shift Prediction. Success in theoretical prediction of NMR chemical shifts is possible due to the development of the "gauge including atomic orbitals approach" (GIAO) that is used for accurate calculations of absolute magnetic shielding tensors of variety nuclei such as ^{1}H, ^{13}C, ^{15}N, and so forth.[21,22] Hartree−Fock (HF) theory is widely used for the prediction of NMR chemical shifts for large-sized molecules, whereas a second-order Møller-Plesset (MP) many-body perturbation theory (MBPT) in combination with GIAO (MP2-GIAO)[23−25] can only be used for medium-sized molecules and highly symmetric large molecules (less than 600 basis functions) because of the poor scalability of the calculations.[26] Highly accurate methods such higher-order MBPT (eg., MP3 and MP4) and methods of coupled cluster theory such as CCSD and CCSD(T) are limited to calculations of NMR chemical shifts of very small molecules only, due to extremely high computational cost.[27] For calculations of the NMR chemical shifts of ILs, density functional theory (DFT) has been the most used approach due to its low cost and acceptable accuracy.[17,28] Bagno et al. predicted the ^{1}H NMR shifts of 1-butyl-3-methylimidazolium tetrafluoroborate ([C_4mim][BF_4]) of a simple ion pair and a cluster of 125 ion pairs using B3LYP/cc-pVTZ and the QM/MM (quantum mechanics/molecular mechanics) approach, respectively.[28] Comparison of the calculated proton NMR shifts of the ion pair to those of the cluster indicated that the cluster results lay much closer to the experimental data. Thus, the H2 proton chemical shifts were significantly affected by extended interionic interactions. In a follow-up paper, the same authors used Car−Parrinello Molecular Dynamics (CPMD) simulations to predict ^{1}H NMR chemical shifts of [C_2mim]Cl. The results showed that compared with the ^{1}H NMR spectrum of the imidazolium cation [C_2mim]$^+$ in a single ion pair, the chemical shifts of the large-scale simulation were again more consistent with experimental data.[28] However, the majority of these predictions for imidazolium-based ILs focused on either the anion effect[17,28] or the solvent effect,[18,29] whereas the effect of quantum chemical method and energetically preferable ion-pair

dx.doi.org/10.1021/jp310267x | J. Phys. Chem. B 2013, 117, 3186−3197

configurations on the accuracy of the calculated proton chemical shifts in the imidazolium ring were not considered in detail.

In this paper, we describe a systematic study of the prediction of proton NMR chemical shifts of a number of ionic liquids (see Scheme 1) incorporating the 1-ethyl-3-methyl-imidazolium cation, C_2mim^+, and anions such as chloride (Cl), tetrafluoroborate (BF_4), hexafluorophosphate (PF_6), acetate (OAc), trifluoroacetate (TFA), dicyanamide (DCA), ethylsulfate ($EtSO_4$), and tosylate (OTs) using a number of wavefunction-based methods such as HF and MP2, as well as DFT-based methods. Proton NMR chemical shifts were calculated for single ion pairs with the view of (1) determining the best quantum chemical method for their accurate prediction and (2) understanding the influence of two energetically preferable ion-pair configurations on chemical shifts of the H2 proton, denoted here as δ(H2), in the imidazolium ring. A two ion-pair cluster approach was also adopted to study changes in the chemical shifts, in which both of these configurations were present simultaneously.

THEORETICAL PROCEDURES

Ion-pair structures of [C_2mim]Cl, [C_2mim][BF_4], [C_2mim][OAc], [C_2mim][DCA], [C_2mim][TFA], [C_2mim][PF_6], [C_2mim][$EtSO_4$], and [C_2mim][OTs] were optimized at the MP2/aug-cc-pVDZ level of theory. The geometries of the C_2mim^+ cation and the ethylsulfate anion were fully conformationally screened at the same level of theory. The optimized geometries are given in the Supporting Information.

The ^{1}H absolute magnetic shielding values were calculated at the following levels of theory: HF, MP2, and various DFT-based methods such as (1) a Becke's three parameter hybrid functional with the Lee−Yang−Parr functional, B3LYP,[30] (2) a hybrid Perdew, Burke, and Ernzerhof functional, PBE1PBE,[31] (3) an extended hybrid functional with the Lee−Yang−Parr correlation functional, X3LYP,[32] (4) a GGA-based functional, mPWPW91,[33] and (5) meta-GGA functionals such as M06−2X,[34,35] and TPSSh.[36] These functionals incorporate the exact HF exchange to a varying degree, starting from as little as 20% for TPSSh to as much as 54% for M06−2X. The long-range corrected functionals such as the coulomb-attenuated hybrid exchange-correlation functional, CAM-B3LYP,[37] and the B97[38] functional augmented with the empirical dispersion correction, wB97XD,[39] were also considered. Five basis sets including 6-311G(d,p), 6-311++G(d,p), 6-311+(3df,2p), cc-pVTZ, and aug-cc-pVTZ were used for HF and B3LYP to study the influence of basis sets on the accuracy of the predicted ^{1}H chemical shifts. The rest of the DFT functionals were employed in conjunction with the 6-311+(3df,2p) basis set. Two basis sets, 6-31+G(d,p) and aug-cc-pVDZ, were used for NMR calculations at the MP2 level of theory. By definition, chemical shifts are found as differences between the calculated absolute magnetic shielding values of protons and those of the reference compound. Chemical shifts of equivalent protons in the cation (e.g., protons in the methyl groups) were found to differ by 1 ppm on average and, therefore, were calculated as an average value. In order to be consistent with the available experimental data, the ^{1}H NMR chemical shifts of the ion pairs were calculated with respect to the magnetic shielding value of twelve equivalent protons in tetramethylsilane (TMS).[40−44] For the sake of consistency, absolute magnetic shielding of protons in TMS was calculated at the same levels of theory as those of the ion pairs. The geometry of TMS was optimized at the MP2/aug-cc-pVDZ level of theory.

Improved electronic energies were performed at the MP2/aug-cc-pVTZ level of theory. The ion-pair binding energy (IPBE) was calculated using the following expression: IPBE = $E_{IP} - E^{min}_{cation} - E^{min}_{anion} + E_{BSSE} + \Delta ZPVE$, where E^{min}_{cation} and E^{min}_{anion} are the electronic energies of the cation and the anion in their lowest energy configurations. A correction factor, E_{BSSE}, arising from the basis set superposition error (BSSE)[45] was introduced to account for the artificial lowering of the binding energy in noncovalent interactions between the cation and anion in the ion pairs. The IPBEs were also corrected for zero-point vibrational energies (ZPVEs).[46]

The following quantum chemical packages were used in the study: *GAUSSIAN 09*[47] for quantum chemical calculations of the proton NMR chemical shifts and *GAMESS-US*[48] for the geometry optimizations.

EXPERIMENTAL PROCEDURES

1-Ethyl-3-methyl Imidazolium Trifluoroacetate ([C_2mim][TFA]). This was made by the carbonate method (halogen free) described in the literature.[49] The reaction typically involves a slow addition of 2.5 g (22.3 mmol) of aqueous solution of trifluoroacetic acid to 8.3 g (44.6 mmol) of 1-ethyl-3-methyl methylcarbonate (50% methanoic) solution. The mixture was stirred for about 1 h at room temperature and then distilled at 70 °C to remove methanol and water. The final product was dried under vacuum, and the yield of a pale yellow liquid was found to be 98%. The product was characterized by electrospray mass spectroscopy for the identification of cations and anions.

Electrospray mass spectroscopy analysis (cone ±25 V): ([C_2mim][TFA]), m/z (relative intensity, %): ES^+, 110.8 ($[C_2mim]^+$, 100); ES^-, 113.1 ($CF_3CO_2^-$, 100). ^{1}H NMR ($CDCl_3$, 300.13 MHz) δ 1.36 (t, 3H, CH_3CH_2), 3.81 (s, 3H, CH_3), 4.12 (q, 2H, CH_3CH_2), 7.38 (s, NCH), 7.36 (s, NCH), 9.75 (s, N2CH).

1-Ethyl-3-methyl Imidazolium Tosylate ([C_2mim][OTs]). This was made by a slow addition of 3.4 g (17.7 mmol) of aqueous solution of *p*-toluenesulfonic acid monohydrate to 6.6 g (35.4 mmol) of 1-ethyl-3-methyl methylcarbonate (50% methanoic) solution. The mixture was stirred for about 1 h at room temperature and then distilled at 70 °C to remove methanol and water. The resulting product, a pale yellow liquid, was dried under vacuum. The yield of the product was found to be 98%. The product was characterized by electrospray mass spectroscopy.

Electrospray mass spectroscopy analysis (cone ± 25 V): ([C_2mim][OTs]) m/z (relative intensity, %): ES^+,110.7 ($[C_2mim]^+$, 100); ES^-, 171.2 $(CH_3C_6H_4SO_3)^-$, 100). ^{1}H NMR ($CDCl_3$, 300.13 MHz) δ 1.40 (t, 3H, CH_3CH_2), 3.87 (s, 3H, NCH_3), 4.17 (q, 2H, NCH_3CH_2), 7.40 (s, NCH), 7.39 (s, NCH), 9.69 (s, N2CH), 7.71 (d, 2H, CCH), 7.1 (d, 2H, CCH), 2.29 (s, 3H, CH_3).

RESULTS AND DISCUSSION

Two energetically preferable configurations (denoted here as Conf. 1 and Conf. 2) were found for the ion pairs of [C_2mim]Cl, [C_2mim][OAc], and [C_2mim][TFA] and are shown in Figure 1. For the rest of the ionic liquids studied only one ion-pair configuration of the anion interacting with the N−C−N motif of the imidazolium ring could be located on

dx.doi.org/10.1021/jp310267x | J. Phys. Chem. B 2013, 117, 3186−3197

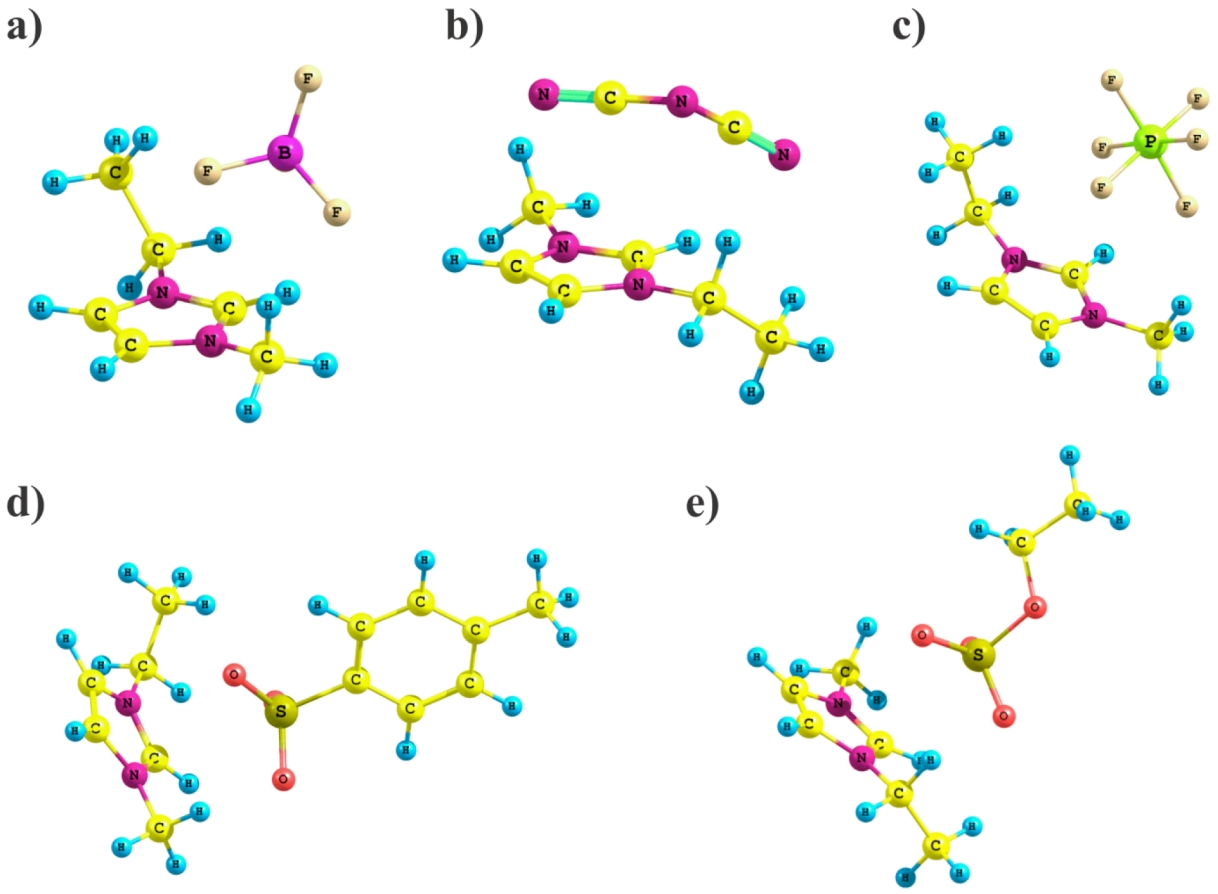

Figure 2. Optimized structures of ion pairs with single configurations: (a) [C_2mim][BF_4], (b)[C_2mim][DCA], (c)[C_2mim][PF_6], (d) [C_2mim][OTs], (e)[C_2mim][$EtSO_4$].

Table 1. Comparison of the ^{1}H NMR Peaks of Imidazolium-Based ILs in Different Solvents

	ref	solvent	H1	H2	H3	H4	H5	H6
[C_2mim][BF_4]	ref 54	neat	3.97	8.35	3.66	7.30	7.23	1.19
	ref 41	$CDCl_3$	4.14	8.55	3.83	7.35	7.41	1.41
	ref 55	acetone-d_6	4.37	8.98	4.03	7.75	7.68	1.54
	ref 56	acetone-d_6	4.388	9.065	4.024	7.757	7.683	1.54
	ref 20	propanone-d_6	4.35	8.88	4.00	7.72	7.65	1.54
[C_4mim][BF_4]	ref 19	neat	4.07	8.53	3.80	7.44	7.39	-
[C_2mim][PF_6]	ref 57	acetone-d_6	4.39	8.96	4.05	7.75	7.68	1.57
	ref 58	$CDCl_3$	4.26	8.82	3.97	7.29	7.24	1.59
[C_4mim][PF_6]	ref 56	neat	4.17	8.75	3.86	7.50	7.50	-
	ref 52	acetone-d_6	4.36	8.97	4.05	7.75	7.70	-

the potential energy surface. The optimized structures are presented in Figure 2.

Sources and Trends in Experimental Chemical Shift Data. To provide a basis for comparison with the calculated chemical shifts in this study, experimental values have been derived from a variety of sources. It has been identified that polar solvents such as water can affect the position of some proton peaks, especially that of the acidic H2 proton in the imidazolium ring. In the study of Balevicius et al.,[50] the chemical shift of the H2, H4, and H5 protons (see Figure 1) were plotted against experimentally measured peaks of the [C_{10}mim]Br ionic liquid dissolved in a number of traditional solvents of increasing dielectric constant from chloroform to deuterated water. The peak of the H2 proton appeared to change by as much as 1 ppm with increasing dielectric constant, whereas changes for the backbone protons were much smaller. For solvents with dielectric constant <20, the H2 peak was shifted by <0.5 ppm, with chloroform showing the least deviation from the neat sample.

Although a number of studies have shown that the ^{1}H NMR spectra of imidazolium-based ionic liquids coupled with BF_4 and NTf_2 anions performed in standard NMR solvents did not differ from those of neat samples,[20,51] measurements of neat ionic liquids can in fact represent a challenge due to their high magnetic susceptibility and occasionally high viscosity, thus producing very broad peaks.[52] For example, the width of the proton peaks in neat [C_2mim]Cl fell in the range of 0.6 to 0.9 ppm.[17] In the study of Rencurosi et al.,[52] a standard NMR tube with a coaxial capillary exhibited low resolution, with the proton peaks being shifted by >1 ppm from those measured using the

dx.doi.org/10.1021/jp310267x | J. Phys. Chem. B 2013, 117, 3186−3197

Table 2. Comparison of Linear Regression Parameters (a,b), Correlation Coefficients (R^2), and Mean Absolute Errors (MAEs) of Proton Chemical Shifts with Respect to Basis Set

			Conf. 1				Conf. 2			
			linear regression				linear regression			
ion pairs	methods	basis set	*a*	*b*	R^2	MAE	*a*	*b*	R^2	MAE
$[C_2mim]Cl$[59]	B3LYP	6-311G(d,p)	1.54	−2.36	0.78	0.88	0.82	0.38	0.99	0.74
		6-311++G(d,p)	1.54	−2.35	0.78	0.91	0.82	0.38	0.99	0.69
		cc-pVTZ	1.62	−2.60	0.77	1.12	0.84	0.32	0.99	0.62
		6-311+G(3df,2p)	1.60	−2.51	0.77	1.12	0.84	0.36	0.99	0.60
		aug-cc-pVTZ	1.61	−2.52	0.77	1.14	0.84	0.36	0.99	0.58
	HF	6-311G(d,p)	1.55	−2.39	0.81	0.91	0.84	0.84	0.99	0.63
		6-311++G(d,p)	1.56	−2.41	0.81	0.95	0.85	0.85	0.99	0.59
		cc-pVTZ	1.62	−2.64	0.79	1.09	0.86	0.86	0.99	0.57
		6-311+G(3df,2p)	1.60	−2.55	0.79	1.09	0.86	0.86	0.99	0.55
		aug-cc-pVTZ	1.62	−2.58	0.79	1.14	0.87	0.87	0.99	0.52
$[C_2mim][OAc]$[40]	B3LYP	6-311G(d,p)	1.40	−1.39	0.73	1.01	1.25	−1.32	0.83	0.20
		6-311++G(d,p)	1.41	−1.36	0.73	1.06	1.25	−1.18	0.84	0.29
		cc-pVTZ	1.45	−1.54	0.73	1.12	1.27	−1.29	0.83	0.32
		6-311+G(3df,2p)	1.45	−1.52	0.73	1.17	1.27	−1.29	0.83	0.35
		aug-cc-pVTZ	1.46	−1.53	0.73	1.18	1.28	−1.29	0.83	0.35
	HF	6-311G(d,p)	1.44	−1.53	0.75	1.11	1.27	−1.28	0.86	0.35
		6-311++G(d,p)	1.44	1.44	0.75	1.16	1.28	−1.28	0.86	0.38
		cc-pVTZ	1.47	−1.68	0.75	1.13	1.29	−1.36	0.86	0.34
		6-311+G(3df,2p)	1.47	−1.64	0.75	1.17	1.29	−1.35	0.86	0.37
		aug-cc-pVTZ	1.48	−1.65	0.75	1.20	1.29	−1.35	0.86	0.38
$[C_2mim][TFA]$	B3LYP	6-311G(d,p)	1.38	−1.17	0.81	1.00	0.90	0.49	0.99	0.05
		6-311++G(d,p)	1.43	−1.50	0.81	1.03	0.90	0.52	1.00	0.04
		cc-pVTZ	1.42	−1.26	0.80	1.10	0.92	0.47	0.99	0.00
		6-311+G(3df,2p)	1.43	−1.50	0.81	1.16	0.92	0.49	0.99	0.02
		aug-cc-pVTZ	1.43	−1.23	0.80	1.16	0.91	0.49	0.99	0.01
	HF	6-311G(d,p)	1.39	−1.16	0.84	1.06	0.95	0.32	1.00	0.05
		6-311++G(d,p)	1.39	−1.11	0.84	1.08	0.95	0.34	1.00	0.05
		cc-pVTZ	1.42	−1.30	0.83	1.08	0.96	0.27	1.00	0.05
		6-311+G(3df,2p)	1.42	−1.26	0.83	1.12	0.96	0.31	1.00	0.06
		aug-cc-pVTZ	1.43	−1.26	0.83	1.15	0.96	0.31	1.00	0.07
$[C_2mim][BF_4]$[41]	B3LYP	6-311G(d,p)					0.99	0.05	0.98	0.03
		6-311++G(d,p)					0.98	0.17	0.98	0.05
		cc-pVTZ					1.00	0.05	0.98	0.04
		6-311+G(3df,2p)					1.00	0.08	0.98	0.07
		aug-cc-pVTZ					1.00	0.07	0.98	0.06
	HF	6-311G(d,p)					1.04	−0.12	0.98	0.08
		6-311++G(d,p)					1.04	−0.09	0.98	0.13
		cc-pVTZ					1.04	−0.16	0.98	0.08
		6-311+G(3df,2p)					1.05	−0.15	0.98	0.12
		aug-cc-pVTZ					1.05	−0.13	0.98	0.12
$[C_2mim][DCA]$[42]	B3LYP	6-311G(d,p)					0.99	0.40	0.97	0.34
		6-311++G(d,p)					0.98	0.41	0.97	0.32
		cc-pVTZ					0.98	0.56	0.96	0.47
		6-311+G(3df,2p)					1.00	0.38	0.96	0.39
		aug-cc-pVTZ					1.00	0.38	0.96	0.40
	HF	6-311G(d,p)					1.04	0.22	0.97	0.45
		6-311++G(d,p)					1.04	0.21	0.97	0.44
		cc-pVTZ					1.05	0.16	0.97	0.45
		6-311+G(3df,2p)					1.05	0.17	0.97	0.46
		aug-cc-pVTZ					1.06	0.17	0.97	0.48
$[C_2mim][PF_6]$[58]	B3LYP	6-311G(d,p)					1.02	−0.32	1.00	0.20
		6-311++G(d,p)					0.93	0.44	1.00	0.06
		cc-pVTZ					1.00	−0.06	0.99	0.07
		6-311+G(3df,2p)					1.00	−0.01	0.99	0.04
		aug-cc-pVTZ					1.01	−0.10	1.00	0.07
	HF	6-311G(d,p)					0.93	0.70	1.00	0.31
		6-311++G(d,p)					0.94	0.64	1.00	0.33

dx.doi.org/10.1021/jp310267x | J. Phys. Chem. B 2013, 117, 3186−3197

Table 2. continued

			Conf. 1				Conf. 2			
			linear regression				linear regression			
ion pairs	methods	basis set	*a*	*b*	R^2	MAE	*a*	*b*	R^2	MAE
		cc-pVTZ					0.99	0.24	1.00	0.17
		6-311+G(3df,2p)					0.99	0.25	0.99	0.20
		aug-cc-pVTZ					0.99	0.22	1.00	0.19
$[C_2mim][EtSO_4]$[44]	B3LYP	6-311G(d,p)					0.84	0.62	1.00	0.29
		6-311++G(d,p)					0.84	0.60	1.00	0.29
		cc-pVTZ					0.87	0.49	0.99	0.27
		6-311+G(3df,2p)					0.87	0.47	0.99	0.25
		aug-cc-pVTZ					0.87	0.50	0.99	0.26
	HF	6-311G(d,p)					0.89	0.44	1.00	0.18
		6-311++G(d,p)					0.90	0.42	1.00	0.16
		cc-pVTZ					0.92	0.28	0.99	0.20
		6-311+G(3df,2p)					0.92	0.27	0.99	0.18
		aug-cc-pVTZ					0.92	0.29	0.99	0.17
$[C_2mim][OTs]$	B3LYP	6-311G(d,p)					0.91	0.39	1.00	0.13
		6-311++G(d,p)					0.91	0.39	1.00	0.14
		cc-pVTZ					0.93	0.27	0.99	0.13
		6-311+G(3df,2p)					0.93	0.25	1.00	0.14
	HF	6-311G(d,p)					0.96	0.19	1.00	0.03
		6-311++G(d,p)					0.96	0.21	1.00	0.01
		cc-pVTZ					0.97	0.07	1.00	0.08
		6-311+G(3df,2p)					0.98	0.07	1.00	0.08

high-resolution magic angle spinning technique. In addition, some ionic liquids have melting points above room temperature, thus preventing measurements of neat liquid samples at RT. For example, $[C_2mim][PF_6]$ melts around 60 °C,[53] and hence, ^{1}H NMR data for this ionic liquid are only available in solvents.

In Table 1 we compare proton peaks of neat $[C_2mim][BF_4]$,[54] $[C_4mim][BF_4]$[19] and $[C_4mim][PF_6]$[53] with those of $[C_2mim][BF_4]$, $[C_2mim][PF_6]$, and $[C_4mim][PF_6]$ measured in various solvents.[20,41,55−58] We expect that the butyl chain in the imidazolium cation should only slightly alter the peak positions of protons compared to the C_2mim-based ILs. As shown in Table 1, the difference in proton peaks is indeed within 0.2 ppm between C_2mim- and C_4mim-based ILs coupled with the same anion. Analysis of Table 1 reveals a common trend that solvents shift proton peaks of the ILs upfield. As expected, the magnitude of the shift depends on dielectric constant of solvent: the lower the dielectric constant, the smaller the shift. Since proton NMR data of high resolution could only be found for neat $[C_2mim][BF_4]$, for the analysis of calculated NMR shifts the preference was given to the literature data taken in the same solvent with a relatively low dielectric constant such as chloroform, as these NMR data are expected to be the closest to those of neat samples. For the C_2mim-based ionic liquids coupled with the tetrafluoroborate,[41] chloride,[59] acetate,[40] dicyanamide,[60] hexafluorophosphate,[58] and ethylsulfate[44] anions, the NMR data came from the literature data in deuterated chloroform solutions, whereas for the ILs in combination with the trifluoroacetate and tosylate anions, the proton NMR spectra were measured in this work (for more detail see Experimental Procedures).

Method and Basis Set Dependence. The calculated NMR chemical shifts of the protons in the imidazolium cation at all levels of theory are presented in the Supporting Information (see Table S1). Two criteria were used to assess the accuracy of the predicted proton chemical shifts in ion pairs: (1) linear regression analysis and (2) mean absolute errors (MAEs). The existence of linear dependence between experimental and calculated proton NMR chemical shifts was established by Katsyuba et al.[29] who used this type of regression to study the quality of the calculated ^{1}H chemical shifts of $[C_2mim][BF_4]$. For the regression analysis, the correlation between the predicted ^{1}H NMR shifts of the six protons in the $[C_2mim]^+$ ring and experimental NMR shifts was fitted to the following linear regression equation:

$$\delta_{calc} = a\delta_{exp} + b \quad (1)$$

The quality of the regression was judged by the linear correlation coefficients, R^2, that should approach 1.0, even when the predicted proton NMR shifts are either systematically underestimated or overestimated; in other words this approach assesses the ability of the calculation to predict the trends and relative shifts of the protons in the cation. Linear regression fit parameters for each ion pair are shown in Tables 2 and 3.

As an alternate approach to assessment of the accuracy of the predictions for each ionic liquid, the mean absolute errors (MAEs) were calculated using the following expression:

$$\mathrm{MAE} = \sum_{i=1}^{N} \frac{|\delta_{calc} - \delta_{exp}|}{N} \quad (2)$$

where δ_{calc} and δ_{exp} are theoretical and experimental chemical shifts in ppm, respectively; and N is the number of nonequivalent protons in the imidazolium cation, i.e., 6. This approach is more sensitive to systematic errors than the linear regression analysis; for example, if the calculated values are all systematically shifted from the experimental, then the MAE will be large even under circumstances where the linear fit is excellent. The MAEs for the protons in the imidazolium cation in both Conf. 1 and Conf. 2 are presented in Table 2 and Table 3, whereas the mean absolute errors of the individual H2 chemical shift in Conf. 2 are shown in Table 4.

dx.doi.org/10.1021/jp310267x | J. Phys. Chem. B 2013, 117, 3186−3197

Table 3. Comparison of Linear Regression Parameters (a and b), Correlation Coefficients (R^2) and Mean Absolute Errors (MAEs) of Proton Chemical Shifts with Respect to the Level of Theory and Ion-Pair Configuration

		Conf 1				Conf 2			
		linear regression				linear regression			
ion pairs	method[a]	a	b	R^2	MAE	a	b	R^2	MAE
$[C_2mim]Cl$[17]	HF	1.60	−2.55	0.79	1.09	0.86	0.29	0.99	0.55
	B3LYP	1.60	−2.51	0.77	1.12	0.84	0.36	0.99	0.60
	CAM-B3LYP	1.61	−2.54	0.77	1.14	0.85	0.37	0.99	0.56
	wB97XD	1.62	−2.32	0.77	1.40	0.84	0.64	0.99	0.30
	TPSSh	1.59	−2.48	0.77	1.07	0.84	0.35	0.99	0.64
	PBE1PBE	1.61	−2.57	0.77	1.12	0.85	0.32	0.99	0.61
	mPWPW91	1.61	−2.58	0.76	1.12	0.84	0.34	0.99	0.65
	M06−2x	1.65	−2.64	0.79	1.31	0.87	0.34	1.00	0.44
	X3LYP	1.60	−2.49	0.77	1.14	0.84	0.36	0.99	0.58
	MP2/6-31+G(d,p)	1.55	−2.22	0.83	1.20	0.84	0.66	0.99	0.27
	MP2/aug-cc-pVDZ	1.58	−2.37	0.80	1.13	0.87	0.36	0.99	0.78
$[C_2mim][OAc]$[40]	HF	1.47	−1.64	0.75	1.17	1.29	−1.35	0.86	0.37
	B3LYP	1.45	−1.52	0.73	1.17	1.27	−1.29	0.83	0.35
	CAM-B3LYP	1.47	−1.57	0.73	1.21	1.29	−1.33	0.84	0.39
	wB97XD	1.47	−1.34	0.73	1.46	1.29	−1.07	0.84	0.64
	TPSSh	1.44	−1.51	0.72	1.13	1.27	−1.28	0.83	0.31
	PBE1PBE	1.46	−1.57	0.73	1.17	1.28	−1.33	0.84	0.35
	mPWPW91	1.45	−1.53	0.72	1.16	1.27	−1.29	0.83	0.29
	M06−2x	1.51	−1.68	0.75	1.37	1.32	−1.36	0.85	0.53
	X3LYP	1.45	−1.51	0.73	1.18	1.28	−1.28	0.83	0.36
	MP2/6-31+G(d,p)	1.44	−1.17	0.76	1.45	1.28	−0.97	0.86	0.71
	MP2/aug-cc-pVDZ	1.47	−1.53	0.75	1.24	1.29	−1.28	0.86	0.45
$[C_2mim][TFA]$	HF	1.42	−1.26	0.83	1.12	0.96	0.31	1.00	0.06
	B3LYP	1.43	−1.50	0.81	1.16	0.92	0.49	0.99	0.02
	CAM-B3LYP	1.43	−1.26	0.81	1.18	0.92	0.47	1.00	0.04
	wB97XD	1.44	−1.04	0.81	1.44	0.93	0.70	0.99	0.30
	TPSSh	1.42	−1.24	0.80	1.12	0.88	0.72	0.99	0.05
	PBE1PBE	1.43	−1.29	0.81	1.15	0.92	0.46	0.99	0.01
	mPWPW91	1.44	−1.29	0.79	1.16	0.91	0.50	0.99	0.00
	M06−2x	1.47	−1.32	0.82	1.32	0.91	0.56	0.99	0.18
	X3LYP	1.43	−1.23	0.80	1.17	0.92	0.46	0.99	0.05
	MP2/6-31+G(d,p)	1.39	−1.06	0.85	1.41	0.96	0.63	1.00	0.41
$[C_2mim][BF_4]$[41]	HF					1.05	−0.15	0.98	0.12
	B3LYP					1.00	0.08	0.98	0.07
	CAM-B3LYP					1.01	0.02	0.98	0.10
	wB97XD					1.02	0.27	0.98	0.36
	TPSSh					1.00	0.07	0.98	0.06
	PBE1PBE					1.01	0.01	0.98	0.07
	mPWPW91					0.99	0.10	0.98	0.05
	M06−2x					1.06	−0.06	0.99	0.25
	X3LYP					1.00	0.08	0.98	0.09
	MP2/6-31G+(d,p)					1.05	0.21	0.98	0.47
$[C_2mim][DCA]$[42]	HF					1.05	0.17	0.97	0.46
	B3LYP					1.00	0.38	0.96	0.39
	CAM-B3LYP					1.01	0.35	0.97	0.42
	wB97XD					1.02	0.59	0.97	0.70
	TPSSh					1.00	0.38	0.96	0.37
	PBE1PBE					1.01	0.34	0.97	0.40
	mPWPW91					0.99	0.42	0.96	0.36
	M06−2x					1.06	0.27	0.97	0.59
	X3LYP					1.00	0.39	0.96	0.41
	MP2/6-31+G(d,p)					1.05	0.51	0.98	0.76
	MP2/aug-cc-pVDZ					1.05	0.26	0.97	0.54
$[C_2mim][PF_6]$[58]	HF					0.99	0.25	0.99	0.20
	B3LYP					1.00	−0.01	0.99	0.04
	CAM-B3LYP					1.02	−0.15	1.00	0.03
	wB97XD					1.02	0.16	0.99	0.25

dx.doi.org/10.1021/jp310267x | J. Phys. Chem. B 2013, 117, 3186−3197

Table 3. continued

		Conf 1				Conf 2			
		linear regression				linear regression			
ion pairs	method[a]	*a*	*b*	R^2	MAE	*a*	*b*	R^2	MAE
	TPSSh					0.97	0.13	0.99	0.01
	PBE1PBE					1.03	−0.27	1.00	0.11
	mPWPW91					1.01	−0.20	0.99	0.14
	M06−2x					1.04	−0.08	1.00	0.11
	X3LYP					1.00	−0.04	0.99	0.03
	MP2/6-31+G(d,p)					1.06	0.06	0.99	0.38
$[C_2mim][EtSO_4]$[44]	HF					0.92	0.27	0.99	0.18
	B3LYP					0.87	0.47	0.99	0.25
	CAM-B3LYP					0.89	0.43	0.99	0.22
	wB97XD					0.89	0.67	0.99	0.05
	TPSSh					0.87	0.46	0.99	0.27
	PBE1PBE					0.88	0.41	0.99	0.25
	mPWPW91					0.86	0.49	0.99	0.28
	M06−2x					0.94	0.33	1.00	0.04
	X3LYP					0.87	0.48	0.99	0.23
	MP2/6-31+G(d,p)					0.91	0.68	1.00	0.19
$[C_2mim][OTs]$	HF					0.98	0.07	1.00	0.08
	B3LYP					0.93	0.25	1.00	0.14
	CAM-B3LYP					0.94	0.22	1.00	0.10
	wB97XD					0.94	0.48	0.99	0.16
	TPSSh					0.93	0.25	0.99	0.15
	PBE1PBE					0.94	0.21	1.00	0.13
	mPWPW91					0.92	0.27	0.99	0.16
	M06−2x					0.98	0.17	0.99	0.06
	X3LYP					0.93	0.26	1.00	0.12
	MP2/6-31+G(d,p)					0.97	0.47	0.99	0.30

[a]The 6-311+G(3df,2p) basis set was used in the calculations, unless specified otherwise.

Table 4. Mean Absolute Errors (MAEs) of the H2 Chemical Shift of the Imidazolium Ring

method	basis set	Conf. 1	Conf. 2
B3LYP	6-311G(d,p)	6.66	0.91
	6-311++G(d,p)	6.69	0.90
	cc-pVTZ	7.28	1.15
	6-311+G(3df,2p)	7.31	1.13
	aug-cc-pVTZ	7.34	1.16
HF	6-311G(d,p)	6.56	0.98
	6-311++G(d,p)	6.61	0.98
	cc-pVTZ	7.24	1.10
	6-311+G(3df,2p)	7.04	1.10
	aug-cc-pVTZ	7.13	1.14
CAM-B3LYP	6-311+G(3df,2p)	7.34	1.15
wB97XD	6-311+G(3df,2p)	7.66	1.43
TPSSh	6-311+G(3df,2p)	7.21	1.08
PBE1PBE	6-311+G(3df,2p)	7.32	1.11
mPWPW91	6-311+G(3df,2p)	7.48	1.13
M06−2x	6-311+G(3df,2p)	7.64	1.31
X3LYP	6-311+G(3df,2p)	7.32	1.14
MP2	6-31+G(d,p)	6.75	1.33
MP2	aug-cc-pVDZ	7.51	1.71

Analysis of Table 2 reveals that *regardless of the ion-pair configuration* the linear correlation coefficients at both HF and B3LYP levels of theory change only slightly, within 0.03, on going from a basis set with no diffuse functions such as 6-311G(d,p) to a heavily augmented basis set such as aug-cc-pVTZ. Surprisingly, the absence of diffuse functions does not significantly affect the proton chemical shifts. The mean absolute errors appear to be rather systematic in the chosen basis set series and fall below 0.5 ppm for Conf. 2. There are a couple of exceptions in this trend. For $[C_2mim][PF_6]$, two Pople-type basis sets, 6-311G(d,p) and 6-311++G(d,p), at both HF and B3LYP levels of theory produce different linear regression coefficients, *a* and *b*, compared to those of the other three basis sets, whereas in the case of $[C_2mim]Cl$, the MAEs for both ion-pair configurations are above 0.5 ppm. Considering the diverse set of ILs studied, it can be concluded that the effect of basis set on the predicted proton NMR spectra of imidazolium-based ILs is rather negligible.

To study the effect of quantum chemical methods on the accuracy of the calculated proton NMR chemical shifts compared to experimental data, the R^2 values calculated with the HF and DFT-based methods in combination with the same basis set, 6-311+G(3df,2p), as well as the MP2 method with the 6-31+G(d,p) and aug-cc-pVDZ basis sets, were compared in Table 3. Analysis of the R^2 magnitudes reveals that all quantum chemical methods chosen in this study produced similar results regardless of the ion-pair configurations, i.e., Conf. 1 and Conf. 2. Out of these methods, HF and MP2 produced marginally larger linear correlation coefficients. Surprisingly, none of the DFT functionals or the MP2 method showed any improvement with respect to HF, indicating that the *proton chemical shifts are insensitive to electron correlation effects*. Among the methods considered, the HF method is a good compromise between cost and accuracy, and therefore, it can be recommended as a method of choice for proton NMR shift calculations of ionic liquids.

dx.doi.org/10.1021/jp310267x | J. Phys. Chem. B 2013, 117, 3186−3197

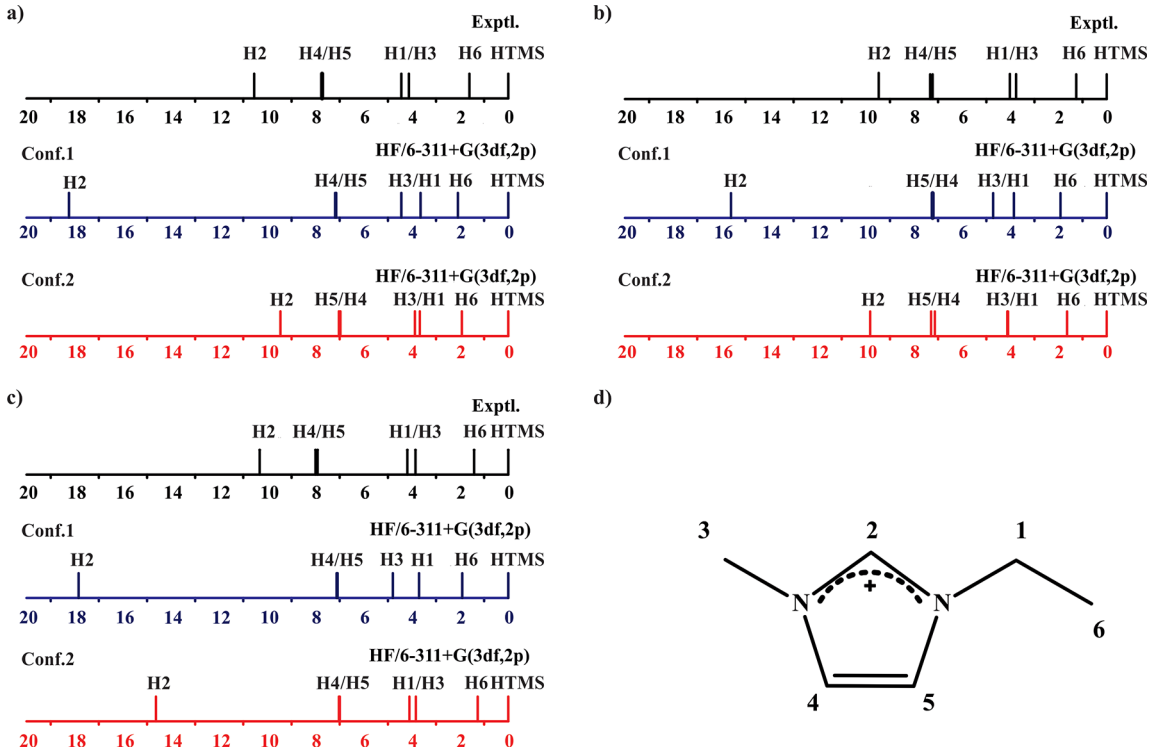

Figure 3. Experimental[17,40,43] (black line) and calculated ^{1}H NMR spectra of ion pairs of Conf. 1 (blue line) and Conf. 2 (red line) (ppm): (a) [C_2mim]Cl; (b) [C_2mim][TFA]; (c) [C_2mim][OAc]; (d) chemical structure of the [C_2mim]$^+$ with carbon atom numbering.

Proton Shifts and Ion-Pair Configurations. From experimental data it is established that the position of the H2 peak is located between 8.55 ppm for [C_2mim][BF_4] and 10.55 ppm [C_2mim]Cl (for more detail, see the Supporting Information). The H2 chemical shifts in the isolated C_2mim$^+$ cation were found to be 7.9 ppm, 8.39 ppm, and 8.5 ppm as calculated with respect to TMS at the B3LYP/6-311+(3df,2p), HF/6-311+(3df,2p), and MP2/aug-cc-pVDZ levels of theory, respectively. This finding clearly indicates that the H2 peak is more dependent on interionic interactions between the ring and the anion.

Tables 2 and 3 show that the linear correlation coefficients for Conf. 2 of [C_2mim]Cl, [C_2mim][TFA], and [C_2mim]-[OAc] at all levels of theory are obviously higher than those of Conf. 1, and the calculated NMR shifts of the former correlate better with experiment. The average value of R^2 for Conf. 2 is 0.94 compared to that of 0.76 for Conf. 1. The MAE values follow the same trend of the correlation coefficients, although there is a greater variation in these values, of up to 0.5 ppm, among the methods for the same ionic liquid. A comparison between the experimental and calculated proton shifts at the HF/6-311+G(3df,2p) level of theory is presented in Figure 3. It is obvious that the H2 proton is the most sensitive to the position of the anion. The predicted chemical shifts of the H2 proton in Conf. 1 move downfield (in the region >15 ppm) compared to the experimental peaks around 10 ppm. In contrast, the predicted δ(H2) values of [C_2mim]Cl and [C_2mim][TFA] in Conf. 2 are located at 9.46 and 9.82 ppm, respectively, thus lying closer to the corresponding experimental data of 10.55 and 9.77 ppm. In the case of [C_2mim][OAc], the theoretical δ(H2) shifts for both Conf. 1 (17.91 ppm) and Conf. 2 (14.63 ppm) are deshielded compared to the experimental peak at 10.32 ppm, with Conf. 2 again being closer to experiment by a few ppm. This trend can be explained by the fact that acetate forms strong hydrogen bonds (<−410 kJ mol^{-1}) with the H2 proton, with the binding energy of Conf. 2 being comparable (within 3 kJ mol^{-1}) to that of the in-plane configuration. Thus, the position of the H2 proton in the NMR spectra of this acetate IL is a more complex mixture of interionic interactions including hydrogen bonding. Analysis of the individual MAEs for the H2 proton in Conf. 2 (see Table 4) further supports the conclusion that Conf. 2 produces better agreement with experimental NMR peaks. The average deviation of δ(H2) of Conf. 2 in all the ILs studies is about 1.15 ppm, varying only slightly within the series of the chosen methods (for more detail, see Figure S1 in the Supporting Information), whereas the MAEs for the H2 proton in Conf. 1 are above 7.16 ppm.

The effect of ion-pair configurations on the other protons in the C_2mim$^+$ ring is much weaker, deviating from experiment by 0.21 ppm on average. Although changing only slightly going from Conf. 2 to Conf. 1, the calculated shifts of the backbone H4 and H5 protons in some ionic liquids are relatively large. For example, the MAEs of the H4, H5, and H6 protons calculated at the HF/6-311+G(3df,2p) level of theory are given for comparison in Figure 4, with the H6 proton representing the same behavior as the other H1 and H3 protons. It is clearly seen that the peak of the H6 proton is in acceptable agreement with experiment for all ionic liquids, whereas the deviations for the backbone protons are 0.57 ppm (Conf. 1) and 0.74 ppm (Conf. 2), and 0.83 ppm (Conf. 1) and 0.93 ppm (Conf. 2) in the chloride and acetate ion pairs, respectively. It is suggested that the backbone protons play an important role in interionic interactions in these cases due to strong hydrogen bonds between the anion and the imidazolium ring.[61] For example, unusually short hydrogen bonds were observed in the crystal structure of [C_2mim]Cl between the H4 and H5 atoms and the chloride anion .[62]

dx.doi.org/10.1021/jp310267x | J. Phys. Chem. B 2013, 117, 3186−3197

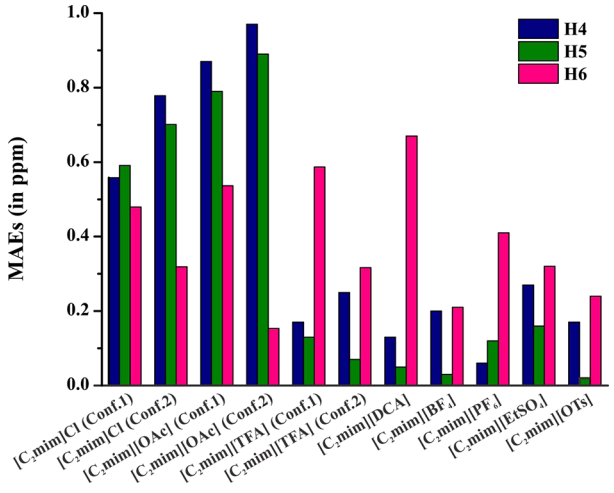

Figure 4. MAEs values of H4, H5, and H6 protons at the HF/6-311+G(3df,2p) level of theory.

Figure 5 shows the relationship between the HF/6-311+G(3df,2p) chemical shifts of the H2 proton and ion-pair

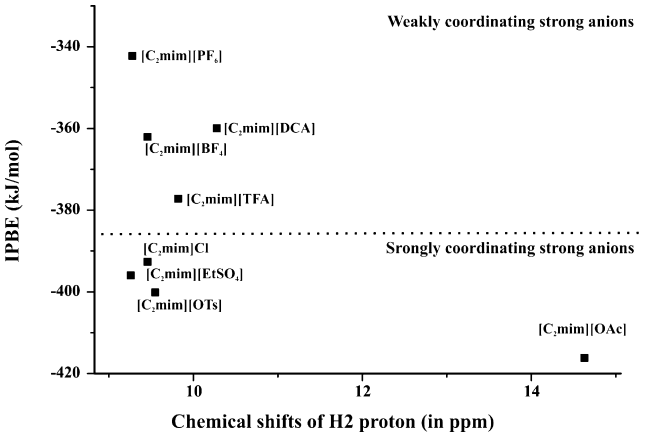

Figure 5. Relationship between the ion-pair binding energies and calculated H2 chemical shifts.

binding energies of Conf. 2 (the lower energy configuration of the two studied). Despite a large range of binding energies (−420 kJ mol^{-1} for acetate to −344 kJ mol^{-1} for PF_6) there appears to be little correlation with chemical shift. The acetate IL appears to be a distinct outlier, for the reasons discussed above.

In the liquid state it is expected that the distance between the cations and anions would be longer than that in the gas-phase ion pair. Therefore, the influence of the distance between the cation and anion in Conf. 1 on the chemical shift of the H2 proton was also studied. The chloride anion and the C_2mim^+ cation were fixed in the same plane and a relaxed scan (i.e., a geometry optimization was performed at each step) was conducted by varying the distance between the C2 atom and Cl^- by the increment of 0.1 Å. The starting C2···Cl distance, R_e, was taken from the optimized geometry of Conf. 1. The increasing distances are denoted here as R_e + 0.1, R_e + 0.2, and so forth, whereas the decreasing distances are denoted as R_e − 0.1, R_e − 0.2, and so forth. The results are presented in Figure 6. It can be clearly seen that, when the distance between the cation and anion increases up to 0.5 Å, the H2 chemical shift approaches that of the experimental value. In contrast, when the C2···Cl distance decreases, the H2 chemical shift moves downfield and, hence, further away from the experimental value (Figure 6). These results indicate that interion distances of >R_e + 0.5 Å could lead to a better agreement between theory and experiment for Conf. 1. Although the interion distances are expected to be longer in the liquid state compared to those in gas-phase structures, it is highly unlikely that the difference will be longer than 0.5 Å.

Using the same strategy, the Cl^- anion was fixed above the plane of the C_2mim^+ cation as in Conf. 2, and a geometry relaxed scan was conducted by varying the distance between the C2 atom and Cl^- by the increment of 0.1 Å. The H2 chemical shift was calculated for each optimized geometry of the scan and the results are presented in Figure 7. It is clear that the decrease in distance between the cation and the anion produces small changes in the H2 chemical shift, whereas the increase in distance leads to further deviation from experiment. Closer analysis of Figure 7 indicates that when the chloride anion moves away from the imidazolium plane within 0.3 Å, δ(H2) changes only slightly within 0.3 ppm. Only a further increase in distance leads to a more significant deviation of >1 ppm. Since the anion−cation distance is not expected to fluctuate above 0.3 Å in the liquid state, the distance effect of Conf. 2 on the H2 chemical shift is expected to be very small.

To summarize, the Conf. 2 ion-pair configuration, in which the anion interacts above the imidazolium ring, provides a good estimate of the H2 chemical shift in the studied ionic liquids, except for [C_2mim][OAc] as explained above. The calculated δ(H2) values of [C_2mim]Cl, [C_2mim][BF_4], [C_2mim][OAc], [C_2mim][DCA], [C_2mim][TFA], [C_2mim][PF_6], [C_2mim]-[$EtSO_4$], and [C_2mim][OTs] vary only slightly with respect to the quantum chemical method and deviate by 0.76 ppm on average from the experimental data. The effect of ion-pair configurations is less significant for other protons in the ring, with the exception of the chloride and acetate anions. It is suggested that for strongly coordinating anions a single ion-pair model might not be sufficient to accurately predict the proton NMR chemical shifts.

Since NMR is a relatively long time-scale measurement, it is expected that the proton NMR spectra will have contribution from all energetically favorable conformations. The results here indicate that the main contributions to the proton NMR spectra could predominantly come from Conf. 2. The effect of larger clusters consisting of eight ion pairs, in which all protons in the ring partake in interionic interactions, as well as solvent effects on the accuracy of predicted proton chemical shifts, should be further investigated and is currently underway.

■ CONCLUSIONS

In conclusion, we predict proton chemical shifts for a series of the imidazolium-based ILs for the two energetically preferable configurations (Conf. 1 and Conf. 2) using wavefunction-based methods such as HF and MP2 and various DFT-based methods. The calculated ^{1}H NMR chemical shifts of ion pairs in Conf. 2, in which the anion interacts from above the imidazolium ring, are in better agreement with experimental data at all levels of theory. In general, the proton NMR chemical shifts do not depend significantly on the basis set and the quantum chemical method used. Therefore, it is recommended to use the HF method for predicting ^{1}H NMR of these types of ions with no sacrifice to accuracy. The chemical shift of the H2 proton was found to strongly depend

dx.doi.org/10.1021/jp310267x | J. Phys. Chem. B 2013, 117, 3186−3197

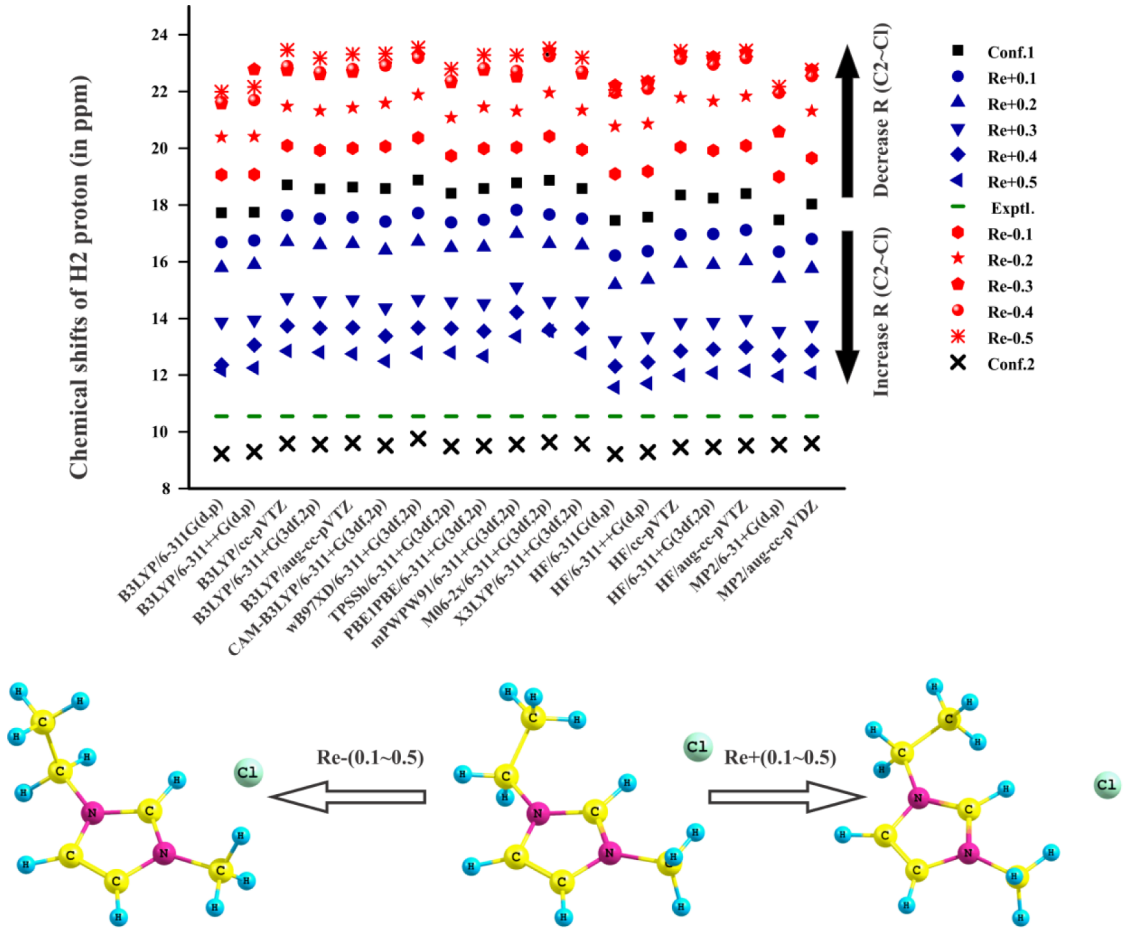

Figure 6. Calculated NMR shifts of the H2 proton in $[C_2mim]Cl$ with varying distance between the C2 atom and the chloride anion in Conf. 1.

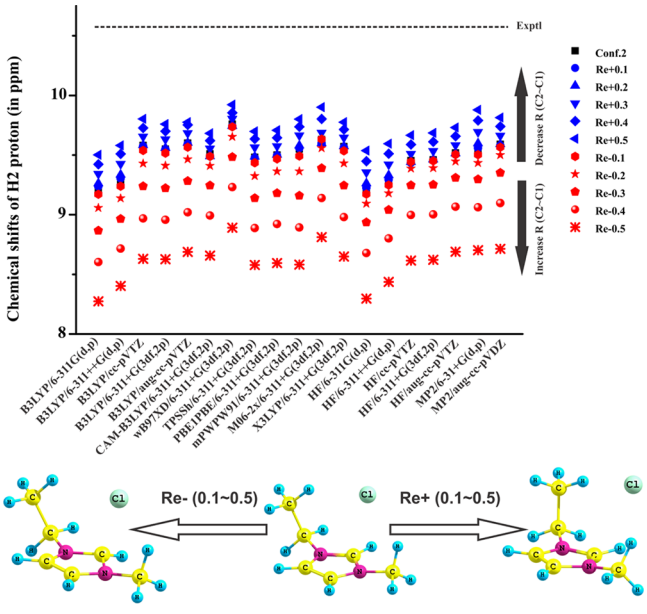

Figure 7. Calculated NMR shifts of the H2 proton in $[C_2mim]Cl$ with varying distance between the C2 atom and the chloride anion in Conf. 2.

on the strength of interionic interaction with the anion, whereas the effect of ion-pair configuration was insignificant on other protons in the ring. Among the rest of the protons, the largest deviations were found for the backbone H4 and H5 protons in the chloride and acetate ion pairs, regardless of the ion-pair configuration. It is suggested that these atoms are affected due to strong bonding with coordinating anions such as acetate and chloride, and therefore, clusters incorporating interactions with the H4 and H5 protons need to be investigated. Therefore, a simple ion-pair model taken in Conf. 2 could already be considered sufficient for the prediction of the proton chemical shifts in imidazolium-based ILs with weakly coordinating anions. Further studies on the effect of larger clusters for strongly coordinating anions, as well as solvent effects on the proton chemical shifts, are currently underway.

■ ASSOCIATED CONTENT

Ⓢ Supporting Information

Proton chemical shift data and geometries of optimized ion pairs and ionic clusters. This material is available free of charge via the Internet at http://pubs.acs.org.

■ AUTHOR INFORMATION

Notes

The authors declare no competing financial interest.

■ ACKNOWLEDGMENTS

The authors would like to acknowledge and sincerely thank the Monash *e*Research Centre and the National Facility of the National Computational Infrastructure for a generous allocation of computational resources. EII and DRM gratefully

acknowledge the support of the Australian Research Council for their Fellowships and a Discovery project grant.

REFERENCES

(1) Ishikawa, M.; Sugimoto, T.; Kikuta, M.; Ishiko, E.; Kono, M. *J. Power Sources* **2006**, *162*, 658−662.
(2) Matsumoto, H.; Sakaebe, H.; Tatsumi, K.; Kikuta, M.; Ishiko, E.; Kono, M. *J. Power Sources* **2006**, *160*, 1308−1313.
(3) Seki, S.; Mita, Y.; Tokuda, H.; Ohno, Y.; Kobayashi, Y.; Usami, A.; Watanabe, M.; Terada, N.; Miyashiro, H. *Electrochem. Solid-State Lett.* **2007**, *10*, A237−A240.
(4) Kawano, R.; Matsui, H.; Matsuyama, C.; Sato, A.; Susan, M. A. B. H.; Tanabe, N.; Watanabe, M. *J. Photochem. Photobiol., A* **2004**, *164*, 87−92.
(5) Seki, S.; Kobayashi, Y.; Miyashiro, H.; Ohno, Y.; Usami, A.; Mita, Y.; Kihira, N.; Watanabe, M.; Terada, N. *J. Phys. Chem. B* **2006**, *110*, 10228−10230.
(6) Izgorodina, E. I. *Phys. Chem. Chem. Phys.* **2011**, *13*, 4189−4207.
(7) Hunt, P. A. *J. Phys. Chem. B* **2007**, *111*, 4844−4853.
(8) Every, H. A.; Bishop, A. G.; MacFarlane, D. R.; Oradd, G.; Forsyth, M. *Phys. Chem. Chem. Phys.* **2004**, *6*, 1758−1765.
(9) Izgorodina, E. I.; Maganti, R.; Armel, V.; Dean, P. M.; Pringle, J. M.; Seddon, K. R.; MacFarlane, D. R. *J. Phys. Chem. B* **2011**, *115*, 14688−14697.
(10) Bonhôte, P.; Dias, A.-P.; Papageorgiou, N.; Kalyanasundaram, K.; Grätzel, M. *Inorg. Chem.* **1996**, *35*, 1168−1178.
(11) Borodin, O. *J. Phys. Chem. B* **2009**, *113*, 12353−12357.
(12) Borodin, O. *J. Phys. Chem. B* **2009**, *113*, 11463−11478.
(13) Fumino, K.; Wulf, A.; Ludwig, R. *Angew. Chem., Int. Ed* **2008**, *47*, 8731−8734.
(14) Izgorodina, E. I.; Rigby, J.; MacFarlane, D. R. *Chem. Commun.* **2012**, *48*, 1493−1495.
(15) Wulf, A.; Fumino, K.; Michalik, D.; Ludwig, R. *ChemPhysChem* **2007**, *8*, 2265−2269.
(16) Stoppa, A.; Hunger, J.; Buchner, R.; Hefter, G.; Thoman, A.; Helm, H. *J. Phys. Chem. B* **2008**, *112*, 4854−4858.
(17) Bagno, A.; D'Amico, F.; Saielli, G. *ChemPhysChem* **2007**, *8*, 873−881.
(18) Palomar, J.; Ferro, V. R.; Gilarranz, M. A.; Rodriguez, J. J. *J. Phys. Chem. B* **2006**, *111*, 168−180.
(19) Suarez, P. A. Z.; Einloft, S.; Dullius, J. E. L.; de Souza, R. F.; Dupont, J. *J. Chim. Phys. Phys. Chim. Biol., 95*, 1626.
(20) D. Holbrey, J.; R. Seddon, K. *J. Chem. Soc., Dalton Trans.* **1999**, 2133−2140.
(21) Wolinski, K.; Hinton, J. F.; Pulay, P. *J. Am. Chem. Soc.* **1990**, *112*, 8251−8260.
(22) J..Grotendorst *Modern Methods and Algorithms of Quantum Chemistry*, 2nd ed.; Mainz, 2000; Vol. 3.
(23) Canongia Lopes, J. N.; Deschamps, J.; Pádua, A. A. H. *J. Phys. Chem. B* **2004**, *108*, 2038−2047.
(24) Canongia Lopes, J. N.; Deschamps, J.; Pádua, A. A. H. *J. Phys. Chem. B* **2004**, *108*, 11250−11250.
(25) Liu, Z.; Huang, S.; Wang, W. *J. Phys. Chem. B* **2004**, *108*, 12978−12989.
(26) Kollwitz, M.; Haser, M.; Gauss, J. *J. Chem. Phys.* **1998**, *108*, 8295−8301.
(27) Karadakov, P. B.; Morokuma, K. *Chem. Phys. Lett.* **2000**, *317*, 589−596.
(28) Bagno, A.; D'Amico, F.; Saielli, G. *J. Phys. Chem. B* **2006**, *110*, 23004−23006.
(29) Katsyuba, S. A.; Griaznova, T. P.; Vidis, A.; Dyson, P. J. *J. Phys. Chem. B* **2009**, *113*, 5046−5051.
(30) Stephens, P. J.; Devlin, F. J.; Chabalowski, C. F.; Frisch, M. J. *J. Phys. Chem.* **1994**, *98*, 11623−11627.
(31) Grimme, S. *J. Comput. Chem.* **2004**, *25*, 1463−1473.
(32) Xu, X.; Goddard, W. A. *Proc. Natl. Acad. Sci. U.S.A.* **2004**, *101*, 2673−2677.
(33) Adamo, C.; Barone, V. *J. Chem. Phys.* **1998**, *108*, 664−675.
(34) Zhao, Y.; Truhlar, D. G. *J. Chem. Phys.* **2006**, *125*, 194101−194101−194118.
(35) Zhao, Y.; Truhlar, D. *Theor. Chem. Acc.* **2008**, *120*, 215−241.
(36) Tao, J.; Perdew, J. P.; Staroverov, V. N.; Scuseria, G. E. *Phys. Rev. Lett.* **2003**, *91*, 146401.
(37) Yanai, T.; Tew, D. P.; Handy, N. C. *Chem. Phys. Lett.* **2004**, *393*, 51−57.
(38) Becke, A. D. *J. Chem. Phys.* **1997**, *107*, 8554−8560.
(39) Chai, J.-D.; Head-Gordon, M. *Phys. Chem. Chem. Phys.* **2008**, *10*, 6615−6620.
(40) Adelwöhrer, C.; Yoneda, Y.; Takano, T.; Nakatsubo, F.; Rosenau, T. *Cellulose* **2009**, *16*, 139−150.
(41) Min, G.-H.; Yim, T.; Lee, H. Y.; Huh, D. H.; Lee, E.; Mun, J.; Oh, S. M.; Kim, Y. G. *Bull. Korean Chem. Soc.* **2006**, *27*, 847−852.
(42) MacFarlane, D. R.; Forsyth, S. A.; Golding, J.; Deacon, G. B. *Green Chem.* **2002**, *4*, 444−448.
(43) Laali, K. K.; Gettwert, V. J. *J. Org. Chem.* **2000**, *66*, 35−40.
(44) Holbrey, J. D.; Reichert, W. M.; Swatloski, R. P.; Broker, G. A.; Pitner, W. R.; Seddon, K. R.; Rogers, R. D. *Green Chem.* **2002**, *4*, 407−413.
(45) Liu, B. *J. Chem. Phys.* **1973**, *59*, 4557.
(46) Grev, R. S.; Janssen, C. L.; Schaefer, H. F., III *J. Chem. Phys.* **1991**, *95*, 5128−5132.
(47) Frisch, M. J.; Trucks, G. W.; Schlegel, H. B.; Scuseria, G. E.; Robb, M. A.; Cheeseman, J. R.; Scalmani, G.; Barone, V.; Mennucci, B.; Petersson, G. A.et al.; *Gaussian 09*, revision A.02; Wallingford, CT, 2009.
(48) Schmidt, M. W.; Baldridge, K. K.; Boatz, J. A.; Elbert, S. T.; Gordon, M. S.; Jensen, J. H.; Koseki, S.; Matsunaga, N.; Nguyen, K. A.; Su, S. *J. Comput. Chem.* **1993**, *14*, 1347−1363.
(49) Zhao, Z.; Ueno, K.; Angell, C. A. *J. Phys. Chem. B* **2011**, *115*, 13467−13472.
(50) Balevicius, V.; Gdaniec, Z.; Dziaugys, L.; Kuliesius, F.; Marsalka, A. *Acta Chim. Slov.* **2011**, *58*, 458−464.
(51) Giernoth, R.; Bankmann, D.; Schlorer, N. *Green Chem.* **2005**, *7*, 279−282.
(52) Rencurosi, A.; Lay, L.; Russo, G.; Prosperi, D.; Poletti, L.; Caneva, E. *Green Chem.* **2007**, *9*, 216−218.
(53) Huddleston, J. G.; Visser, A. E.; Reichert, W. M.; Willauer, H. D.; Broker, G. A.; Rogers, R. D. *Green Chem.* **2001**, *3*, 156−164.
(54) Takao, K.; Tsubomura, T. *J. Chem. Eng. Data* **2012**, *57*, 2497−2502.
(55) Park, S.; Kazlauskas, R. J. *J. Org. Chem.* **2001**, *66*, 8395−8401.
(56) Zhao, X.; Hu, L.; Geng, Y.; Wang, Y. *J. Mol. Catal., A: Chem.* **2007**, *276*, 168−173.
(57) Yoshida, Y.; Saito, G. *J. Mater. Chem.* **2006**, *16*, 1254−1262.
(58) Lin, S.-T.; Ding, M.-F.; Chang, C.-W.; Lue, S.-S. *Tetrahedron* **2004**, *60*, 9441−9446.
(59) Compounds, S. D. f. O.
(60) De Los Ríos, A. P.; Hernández-Fernández, F. J.; Martínez, F. A.; Rubio, M.; Víllora, G. *Biocatal. Biotransform.* **2007**, *25*, 151−156.
(61) Izgorodina, E. I.; MacFarlane, D. R. *J. Phys. Chem. B* **2011**, *115*, 14659−14667.
(62) Elaiwi, A.; Hitchcock, P. B.; Seddon, K. R.; Srinivasan, N.; Tan, Y.-M.; Welton, T.; Zora, J. A. *J. Chem. Soc., Dalton Trans.* **1995**, 3467−3472.